

# Fe<sub>3</sub>O<sub>4</sub>/rice husk/ polypyrrole nanocomposite as a sorbent for efficient lead removal

Mohammad Daneshpazhooh\*

Department of Chemistry, PayameNoor University, PO BOX19395-4697, Tehran, IRAN

Received: 21 June 2024 Accepted: 6 September 2024

DOI: [10.30473/IJAC.2026.77082.1335](https://doi.org/10.30473/IJAC.2026.77082.1335)

## Abstract

Heavy metal pollution, particularly lead (Pb<sup>2+</sup>), poses a significant threat to the environment and human health. In this study, Fe<sub>3</sub>O<sub>4</sub>/rice husk/ polypyrrole (Fe<sub>3</sub>O<sub>4</sub>/Rh/PPy) nanocomposite was synthesized and used for removal of lead from aqueous solutions. In the first, Fe<sub>3</sub>O<sub>4</sub> magnetic nanoparticle was prepared through a simple and one step method and then polypyrrole (PPy) was synthesised chemically on the surface of nanoparticle. FeCl<sub>3</sub> was used as chemical oxidants for oxidation of pyrrole to PPy. The new nanocomposite was characterized by FT-IR, SEM and Dynamic Light Scattering method. The effect of pH, contact time, adsorbent dose, initial concentration, ionic strength and the effect of temperature on the adsorption was checked out in a batch process. Optimal adsorption conditions were determined at pH~ 7, 0.04 g dosage, 45 min contact time, and 30 ppm initial lead concentration, yielding a maximum lead removal efficiency of 99.7 %. Using the equilibrium constants obtained at different temperatures, the thermodynamic parameters were calculated and showed that the uptake of lead is spontaneous and exothermic. The maximum adsorption capacity by using Langmuir equation was calculated 85.47 mg/g. The kinetic data followed by Pseudo second.

**Keywords:** Fe<sub>3</sub>O<sub>4</sub>/rice husk/ polypyrrole nanocomposite, Removal, Lead

## 1. INTRODUCTION

Water is the most essential resource for sustaining life on Earth. As a result, providing clean water is crucial. Due to rapid urbanization, population growth, economic expansion, and industrialization, water contamination is increasing globally. Industrial wastewater has emerged as a significant environmental concern. Heavy metal contamination is one of the most serious environmental problems caused by inappropriate waste disposal from untreated industries. Lead is of particular concern, as metal finishing, electroplating, battery manufacturing, painting, pigments, and other processes are the primary sources of lead [1].

Lead ions are specifically utilized in many industrial processes, including the manufacturing of lead-acid batteries, ammunition, and industrial and medical uses such textile dyeing and metal mining and processing [2,3]. However, a number of health issues, including as cancer, neurological damage, anemia, angioedema, stomachaches, and muscle weakness, can be brought on by high amounts of lead ions in drinking water [4-6]. The World Health Organization (WHO) suggests that drinking water has a maximum lead ions content

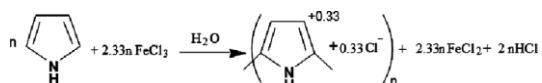
of 0.01 mg/L[7-10]. The result demonstrated that any trace of lead ion in water greater than 0.01 mg/L needs to be removed [11-13]. Several technologies are in use for lead removal. These technologies include ion exchange, chemical precipitation, electrolysis, membrane separation and adsorption. Amongst these, adsorption is more reliable and promising owing to its efficiency, local availability of adsorbents, operational simplicity, cost effectiveness and regeneration potential of the adsorbents [14-17]. Nanoparticles are a new group of materials that emphasized for the environmental treatment due to their unique properties such as large surface area and pore size, small particle size, surface charge, magnetic property, thermal stability, chemical inertness and biocompatibility [18].

Nanotechnology has emerged as a powerful tool for heavy metal remediation, offering efficient and sustainable solutions for removing toxic metals. Several studies have reported the removal of lead from water and wastewater using nanosorbents [19-26]. All of these studies revealed that novel applications of nanomaterials for the removal of lead from water. However, so far, there are no reports showing whether magnetic (Fe<sub>3</sub>O<sub>4</sub>/Rh/PPy)

\* Corresponding author:

E-mail: fatemehsaber2003@pnu.ac.ir

nanocomposite can be used for removal of lead. PPy and its derivatives can be readily synthesized chemically on the surface of different solid substrates such as fibers, glass, cloth, paper as powders, disperse or colloid. Iron (III) chloride has been found to be the best chemical oxidant and water is the best solvent for chemical polymerization [27]. Polymerisation of PPy with ferric chloride as oxidant is given in Fig. 1.



## 2. EXPERIMENTAL

### 2.1. Materials and methods

The chemicals used were all AR grade.  $\text{Fe}(\text{NO}_3)_3 \cdot 9\text{H}_2\text{O}$  (99% wt), rice husk (80-mesh),  $\text{Pb}(\text{NO}_3)_2$  (99% wt),  $\text{NaOH}$  (99.5% wt),  $\text{Na}_2\text{SO}_4$  (95% wt),  $\text{NaCl}$  (99% wt), Ammonia solution 25%,  $\text{FeCl}_3$  and Pyrrole (all from Merck Co, Germany). Standard solutions of lead ions (1000 ppm) were prepared by dissolving of  $\text{Pb}(\text{NO}_3)_2$  salt in the distilled water. A SensAA GBC (Dandenong, Australia) atomic absorption spectrometer was used for measurement of lead in air-acetylene flame. A mechanical shaker KS 130 basic (Deutschland, Germany) having speed control and timer was used for batch experiments. A Metrohm pH meter (Herisau, Switzerland) was employed for pH measurements. The concentrations of the lead solutions were obtained using data from a standard calibration curve.

### 2.2 Preparation of $\text{Fe}_3\text{O}_4/\text{Rh}$

Rice husk(Rh) was supplied from the local market in Kerman and were ground with a household blender until very smooth fine powder was obtained. The particles were passed through an 80-mesh sieve, washed with distilled water and dried in 25 °C. In order to prepare magnetic  $\text{Fe}_3\text{O}_4/\text{Rh}$ , 3.0 g rice husk as a reducing agent was added to 100 ml water containing 4.0 g  $\text{Fe}_3\text{O}_4 \cdot 9\text{H}_2\text{O}$  and the mixture is stirred vigorously for 1 h at 90 °C for reduction of  $\text{Fe}^{3+}$  ions to  $\text{Fe}^{2+}$  ions. Then the pH value of the solution was adjusted to about 10 by gradually addition of ammonia 25% solution with continuing vigorous stirring on the heater stirrer. The freshly formed  $\text{Fe}_3\text{O}_4/\text{Rh}$  NPs were decanted with the help of a handheld magnet. Subsequently, the material was washed with deionized water, dried in at 60 °C and stored for subsequent modification.

### 2.3. Preparation of $\text{Fe}_3\text{O}_4/\text{Rh}/\text{PPy}$ nanocomposite

Pyrrole distilled before polymerisation. Polymerisation was carried out in aqueous solution. In order to prepare  $\text{Fe}_3\text{O}_4/\text{Rh}/\text{PPy}$  nanocomposite(sorbent), 3.0 g of  $\text{Fe}_3\text{O}_4/\text{Rh}$

was dispersed in 80 mL distilled water for 20 min. Then, 6.0 g  $\text{FeCl}_3$  and 0.8 mL freshly distilled pyrrole solution was added to the suspension, with continuing stirring at room temperature on magnetic stirring. After 3 h, the suspension decanted with a magnet. Subsequently, the sorbent was washed with deionized water, dried in at 60 °C for 12 h and then saved for adsorption studies.

### 2.4. Characterization

The functional groups of  $\text{Fe}_3\text{O}_4/\text{Rh}/\text{PPy}$  nanocomposite were identified by FT-IR spectrum in the wave number range of 500–4000  $\text{cm}^{-1}$  by using pressed KBr pellets. The microstructure of the prepared nanocomposite was observed by Scanning Electron Microscopy (SEM) (Cam Scan MV2300). The Dynamic Light Scattering (DLS) test was also employed to specify the average particle size, also.

### 2.5 Adsorption method

Adsorption experiments were conducted in batch system at room temperature by shaking 0.04 g of the sorbent with 25 ml of the aqueous solutions 30 ppm of lead in stoppered pyrex glass flask, at a fixed temperature. The initial pH of the solutions was adjusted with diluted  $\text{HNO}_3$  or  $\text{NaOH}$  0.1 M solution and the shaking speed was 200 rpm for 45 min. At the end of the adsorption period, the sorbent was separated from the suspension with magnetic field out and the lead concentration was determined using FAAS.

The amount of  $\text{Pb}(\text{II})$  ions adsorbed and percentage of removal of  $\text{Pb}(\text{II})$  ions (Re%) was calculated using Equations (1) and (2).

$$q_e = V(C_0 - C_e)/M \quad (1)$$

$$\text{Re\%} = [(C_0 - C_e)/C_0] \times 100 \quad (2)$$

As  $q_e$  is the amount of adsorbed  $\text{Pb}(\text{II})$  ion per gram of the adsorbent,  $C_0$  is initial concentration and  $C_e$  is the equilibrium concentration of the  $\text{Pb}(\text{II})$  ( $\text{mg L}^{-1}$ ) that is obtained from calibration curve and  $M$  is the mass of nanocomposite (g).

## 3. RESULTS AND DISCUSSION

### 3.1 Characterization of the sorbent

$\text{Fe}_3\text{O}_4/\text{Rh}/\text{PPy}$  nanocomposite was characterized employing various techniques including FT-IR, SEM and DLS. FT-IR spectrum of the sorbent is shown in Fig. 2. The peaks around 1531 and 1455  $\text{cm}^{-1}$  correspond to the symmetric and asymmetric C-N and C-C ring-stretching modes of polypyrrole, respectively. Absorption band at 3406  $\text{cm}^{-1}$  is due to the N-H group of polypyrrole. These peaks indicate the doping state of PPy on the nano particle magnetic. SEM analysis was done to identify

the surface and morphology of  $\text{Fe}_3\text{O}_4/\text{Rh/PPy}$  nanocomposite. SEM image of  $\text{Fe}_3\text{O}_4/\text{Rh}$  showed (Fig. 3) that  $\text{Fe}_3\text{O}_4$  nanoparticles incorporate on the surface of rice husk as agglomerated form and other places also. These  $\text{Fe}_3\text{O}_4$  nps are spherical in shape and prepared using rice husk powder as reducing agent.

The Dynamic Light Scattering (DLS) test was also employed to specify the average particle size where its results are available in Fig. 4. Accordingly, the average particles size after incorporating of the PPy was less than 100 nm.

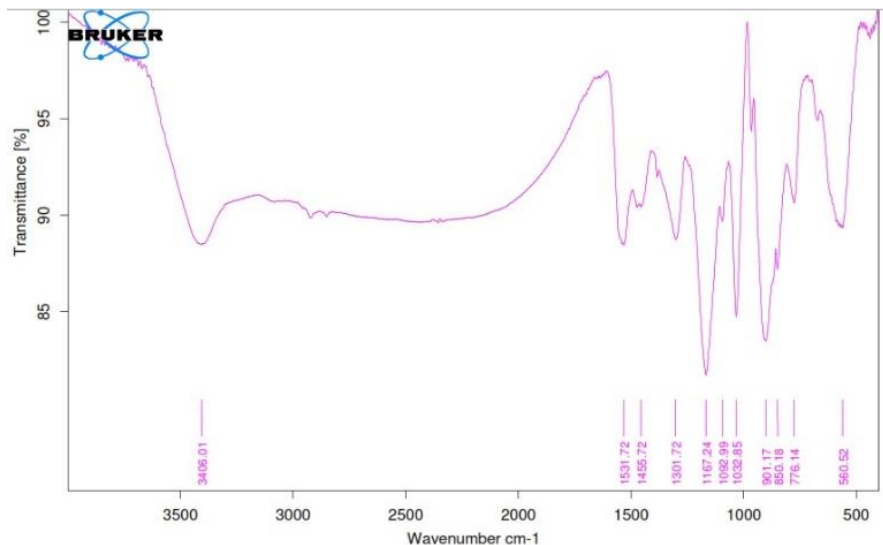


**Fig. 2.** FT-IR spectrum of  $\text{Fe}_3\text{O}_4/\text{Rh/PPy}$  nanocomposite.

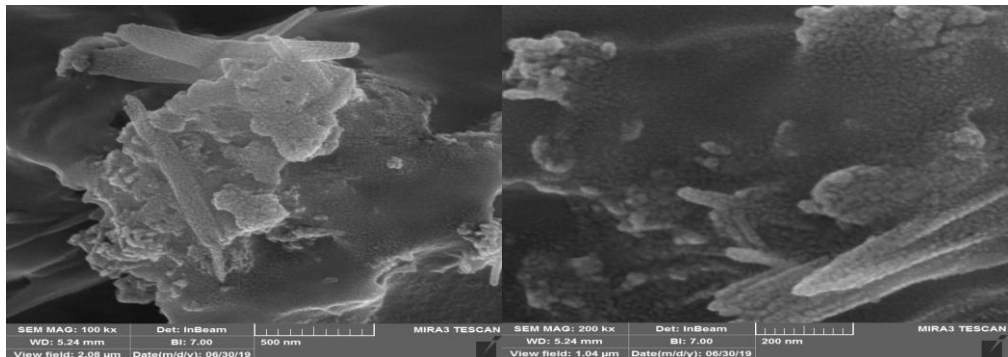


**Fig. 3.** SEM images of  $\text{Fe}_3\text{O}_4/\text{Rh/PPy}$  nanocomposite.

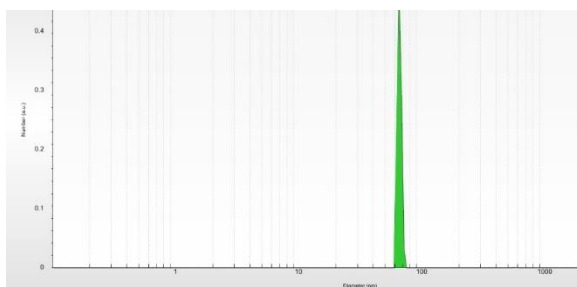


**Fig. 4.** DLS spectrum of nanocomposite.

### 3.2. Effect of pH

pH is a deciding factor for any kind of metal sorption on sorbents in an aqueous solution. The surface properties of sorbents, ionic state of functional groups and species of metals are dependent on pH condition. To find out the proper water condition with maximum metals adsorption pH dependent experiments are needed. The affinity of adsorbent functional sites for lead ions depends on the initial pH of the solution. Lead occurs as  $\text{Pb}^{2+}$ ,  $\text{Pb}(\text{OH})^+$  and  $\text{Pb}(\text{OH})_2$  species in deionized water. The effect of pH on adsorption of

Pb(II) ions was studied over a pH range of 1-8 at room temperature. According to the results depicted in Fig. 5, in acidic range, functional groups on the sorbent protonated and caused electrostatic repulsion to Pb<sup>2+</sup> ions. The percentage of removal of lead increased with increasing pH, due to electrostatic attractions occur between cationic Pb<sup>2+</sup> ions and anionic adsorbent surface. At high pHs, Precipitation occurs due to forming lead hydroxide, therefore, the experiments were performed at pH ~7.

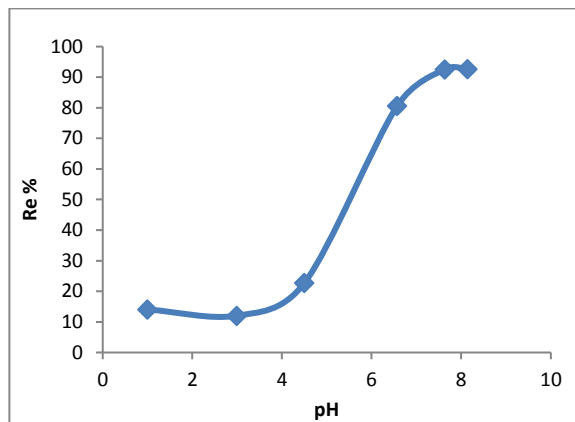


**Fig. 5.** Effect of pH on the removal of lead.

### 3.3. Effect of sorbent dose

Effect of adsorbent dosage on the uptake of lead was studied and is shown in Fig. 6. The percent removal of lead increased from 54.9% to 97.5% with an increase in adsorbent amount. The removal of lead at  $m > 0.04$  g remains almost constant. An increase in the removal with the adsorbent dosage can be attributed to greater surface area and the availability of more adsorption sites. At  $m < 0.04$  g, the adsorbent surface becomes saturated with lead and the residual concentration in the solution is large. Thus, the dose of the adsorbent was fixed to 0.04 g for the subsequent adsorption experiment.

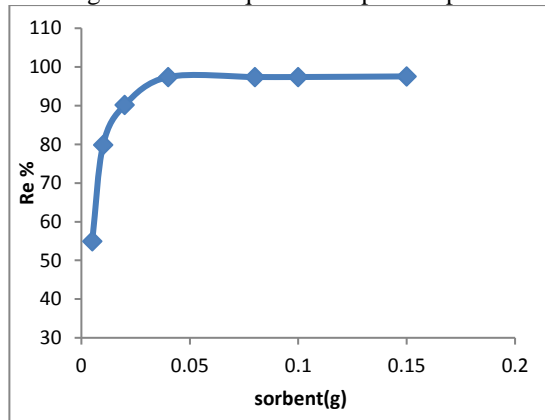


**Fig. 6.** Effect of adsorbent dosage on the removal of lead.

### 3.4. Effect of contact time

Another important characteristic determining whether or not the use of a given adsorbent is feasible for a particular task is the time. The effect of contact time is depicted in Fig. 7. The experiments were performed by varying contact time (1–120 min.) with initial Pb(II) concentration 30mg/L, keeping all other parameters constant. The percent removal increased from 60.7% to 99.1% onto nanocomposite with increasing time. Pb(II) removal increased continuously upto 45 min and then removal efficiency remains constant. This may be attributed that initially, the active sites for Pb(II) ions are available in excess, but after time equilibrium attained due to the saturation of the sorbent active sites. 45 min was selected for more experiments.

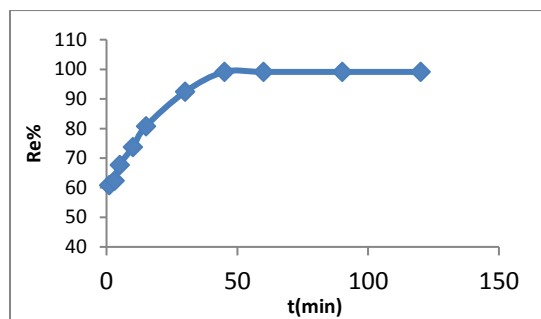


**Fig. 7.** Effect of contact time on lead adsorption.

### 3.5. Effect of temperature

The effect of temperature on the adsorption of lead was studied by varying temperature in the range of 0–45°C. The lead removal decreased with increase in temperature illustrating that adsorption of lead on the sorbent is exothermic. The Gibbs free energy change,  $\Delta G^0$ , is fundamental criterion of spontaneity. The sorption process of lead can be summarized by the following reversible process. The equilibrium constant ( $K_c$ ) is defined as:

$$K_c = (C_0 - C_e)/C_e \quad (3)$$

where  $C_e$  is the concentration of lead at equilibrium. The  $K_c$  value is used in the following equation to determine the  $\Delta G^0$  of sorption.

$$\Delta G^0 = -RT\ln K_c \quad (4)$$

The enthalpy ( $\Delta H^0$ ) and entropy ( $\Delta S^0$ ) can be calculated from the slope and intercept of Vant Hoff equation of  $\Delta G^0$  versus T.

$$\Delta G^0 = \Delta H^0 - T \Delta S^0 \quad (5)$$

R the gas constant ( $8.314 \text{ J mol}^{-1}\text{K}^{-1}$ ) and T is the absolute temperature (K). The obtained  $\Delta G^0$  values and the adsorption thermodynamic parameters are given in Table 1. The positive value  $\Delta S^0$  shows the increase in degree of freedom or increase the disorder of adsorption lead on the sorbent and the negative value  $\Delta H^0$  indicates that adsorption process is exothermic.

**Table 1.** Thermodynamic Parameters of lead.

T (K)	$\Delta G^0$ (J mol <sup>-1</sup> )	$\Delta S^0$ (J mol <sup>-1</sup> K <sup>-1</sup> )	$\Delta H^0$ (kJ mol <sup>-1</sup> )
273	-11171.3		
283	-10723.6	56.15	-26.66
296	-10282.4		
303	-9828.41		
308	-9431.34		
313	-9114.12		
318	-8494.71		

### 3.6. Equilibrium adsorption isotherms

The adsorption isotherms of lead on  $\text{Fe}_3\text{O}_4/\text{Rh/PPy}$  were examined in the concentration range 30-150 mg. L<sup>-1</sup> using Langmuir and Freundlich models to understand the adsorption mechanism. Linear forms of Langmuir and Freundlich isotherms are given in Eqs. (6) and (7).

$$C_e/q_e = (1/Qb) + (1/Q) C_e \quad (6)$$

$$\log q_e = \log K_f + 1/n \log C_e \quad (7)$$

$q_e$  is the amount of adsorbed ion per gram of the adsorbent,  $b$  is Langmuir constant and  $Q$  is adsorption capacity expressed in mg g<sup>-1</sup>,  $n$  is the Freundlich constant, and  $K_f$  is the adsorption coefficient. The results showed the Freundlich model yields somewhat better fit for adsorption of lead (Fig. 8). All the calculated parameters from intercept and slope of plots according to Eqs. (6) and (7) are listed in Table 2.

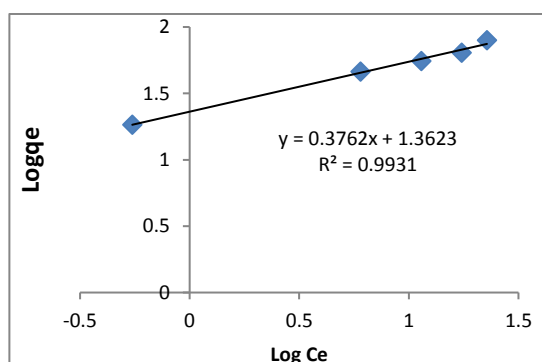
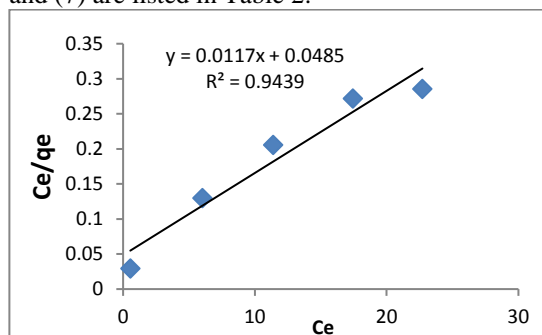


Fig. 8. Langmuir and freundlich isotherms of lead.

**Table 2.** Langmuir and freundlich isotherm constants for lead.

T (K)	Langmuir isotherm		Freundlich isotherm			
	Q(mg g <sup>-1</sup> )	b( L mg <sup>-1</sup> )	R <sup>2</sup>	K <sub>f</sub>	1/n	R <sup>2</sup>
298	85.47	0.24	0.94	23	0.37	0.99

### 3.7. Effect of ionic strength

The effect of various amounts of NaCl and Na<sub>2</sub>SO<sub>4</sub> on the sorption of lead on the nanocomposite was examined. It was seen that the there was no significant decrease in the percent removal efficiency. As, even at high concentration of the salt,  $\text{Fe}_3\text{O}_4/\text{Rh/PPy}$  nanocomposite still has big percent removal efficiency and can be used to efficiency remove lead from aqueous solutions.

### 3.8. Adsorption kinetics

The adsorption kinetics described by the relationship between lead uptake and contact time that is discussed by Pseudo-First order and Pseudo-Second order, Eqs. (8,9).

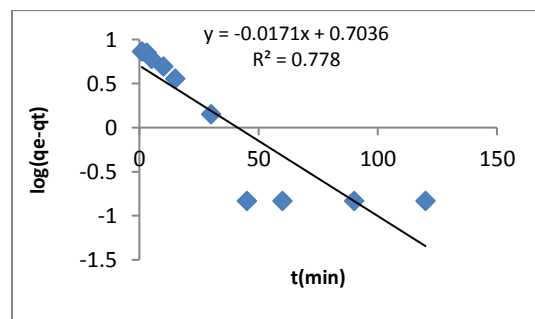
The Pseudo- First order equation is:

$$\log(q_e - q_t) = \log q_e - (k_1 / 2.303) t \quad (8)$$

And the Pseudo-Second order equation is:

$$(t/q_t) = (1/k_2 . q_e^2) + t / q_e \quad (9)$$

where  $q_t$  is the amount of lead adsorbed at 't' time (mg/g),  $t$  is the contact time (min),  $q_e$  is the amount of lead adsorbed at equilibrium (mg/g),  $k_1$  is the rate constant of Pseudo-First order reaction (min<sup>-1</sup>) and  $k_2$  is the rate constant of Pseudo-Second-order reaction (g mg<sup>-1</sup> min<sup>-1</sup>). The slope and intercept of plot of  $\log(q_e - q_t)$  against time (min) were used to determine the First order rate constant  $k_1$ . It was observed that correlation coefficient ( $R^2$ ) was low and experimental data are not fitted well for Pseudo-First order reaction. Hence, the adsorption mechanism cannot be well described by Pseudo-First order kinetics. The Pseudo-Second order rate constant  $k_2$  was calculated from the slope and intercept of the plot  $t/q_t$  against time (Fig. 9). The calculated  $q_e$  ( $q_{e,cal}$ ) was in good agreement with experimental  $q_e$  ( $q_{e,exp}$ ) with correlation coefficient high. These results confirm the well fitting of Pseudo-Second order model for adsorption of lead on to the ( $\text{Fe}_3\text{O}_4/\text{Rh/PPy}$ ) nanocomposite.



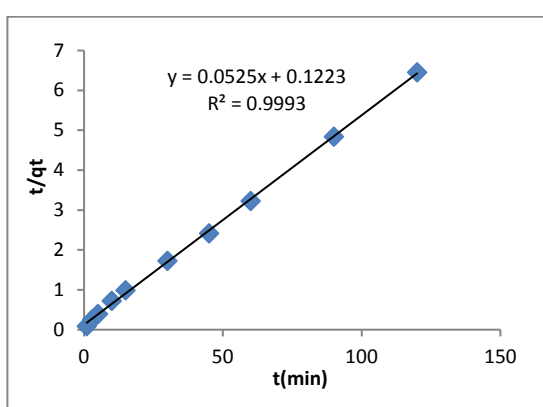


**Fig. 9.** Pseudo-First order and Pseudo-Second order plot for lead adsorption

#### 4. CONCLUSION

In the present paper, a novel sorbent, magnetic  $\text{Fe}_3\text{O}_4/\text{Rh/PPy}$  nanocomposite, was synthesized and used to remove lead ions efficiently from aqueous solutions. In the first, magnetic nanoparticles were synthesized using rice husk as the reducing agent and then the nanocomposite prepared with incorporation PPy. The nanocomposite exhibited high adsorption and purification efficiency, achieving 99.7% removal of lead ions at pH~7. The results revealed that adsorption time and pH value are significant factors. The optimal conditions were: contact time of 45 min, a pH~7, dose of sorbent, 0.04g based on the results. The removal of lead ions using  $(\text{Fe}_3\text{O}_4/\text{Rh/PPy})$  nanocomposite proved great potential as an effective sorbent for lead removal from aqueous solutions.

#### Acknowledgments

The authors would like to express their appreciations to Payame Noor University of Kerman for providing research facilities. This research was supported by the Research Laboratory of Payame Noor University of Kerman.

#### References

- [1] T.A. Abdullah, AH. Abdalsalam, A.A. Ati, R. T. Rasheed, S. Al-Anssari, Novel  $\text{CoCdFe}_2\text{O}_4/\text{Chitosan-PANi}$  ternary nanocomposite for High-Efficiency Lead Removal. *J. Solid State Chem.* 355 (2026) 125794.
- [2] S. Babel, T.A. Kurniawan, Low-cost adsorbents for heavy metals uptake from contaminated water: a review. *J. Hazard. Mater.* 97 (2003) 219-243.
- [3] M.A. Taleb, Nanostructured aerogels for adsorptive removal of pharmaceutical pollutants from wastewater: a review on synthesis and application. *J. Environ. Chem. Eng.* (2024) 114538.
- [4] A. Ara, J.A. Usmani, Lead toxicity: a review. *Interdiscip. Toxicol.* 8 (2) (2015) 55-64.
- [5] A.A. Ramírez-Coronel, Hospital wastewater treatment methods and its impact on human health and environments. *Rev. Environ. Health* 39 (3)(2024) 423-434.
- [6] R. Moradi, Study of  $\text{Fe}_3\text{O}_4/\text{ZnO}$  nanocomposite efficiency in Ponceau 4R dye photodegradation process and optimization of operational parameters. *Iran. J. Chem. Chem. Eng. (IJCCE) Res. Artic.* 43 (11) (2024).
- [7] N. Ul Haq, Drinking water: a major source of lead exposure in Karachi, Pakistan. *EMHJ-East. Mediterr. Health J.* 17(11)(2011) 882-886.
- [8] B. Tessema, Synthesis and characterization of biosilica gel produced from teff (Eragrostis tef) straw using the sol-gel technique. *Bioresour. Technol.* 22(2023) 101497.
- [9] B. Tessema, G. Gonfa, S. Mekuria, Preparation of modified silica gel supported silver nanoparticles and its evaluation using zone of inhibition for water disinfection. *Arab. J. Chem.*, (2024) 106036.
- [10] B. Tessema, Synthesis and evaluation of the anti-bacterial effect of modified silica gel supported silver nanoparticles on *E. coli* and *S. aureus*. *Results Chem.* 7(2024) 101471.
- [11] B. Tessema, Characteristic investigations on bio-silica gel prepared from teff (eragrostis tef) straw: effect of calcination time. *Mater. Res. Express* 10 (11)(2023) 115102.
- [12] B.T. Asfaw, K.B. Gebeyehu, Production of waste animal bone as a heterogeneous solid base catalyst for transesterification of *Jatropha* oil. *Int. J. Chem. Sep. Technol.* 5 (1) (2019) 28-48.
- [13] S.S. AlNeyadi, Phosphazene-based covalent organic framework: advanced leadcapture material with visual indicator for efficient water purification. *J. Hazard. Mater. Adv.* 17 (2025) 100593.
- [14] L.F. Musico, C.M. Santos, M.L.P. Dalida, and D.F.R. Rodrigues, Improved removal of lead(II) from water using a polymer-based graphene oxide nanocomposite, *J. Mater. Chem.* (2013) 3789-3796.

[15] S. Kumar, R.R. Nair, P.B. Pillai, S.N. Gupta, M.A.R. Iyengar, and A.K. Sood, Graphene oxide MnFe<sub>2</sub>O<sub>4</sub> magnetic nanohybrids for efficient removal of lead and arsenic from, *water. Appl. Mater. Interf.* 6(2014) 7426-17436.

[16] S. Joshi, V.K. Garg, J. Saini, and K. Kadirvelu, Removal of toluidine blue O dye from aqueous solution by silica-iron oxide nanoparticles, *Mater. Focus.* 7 (2018) 140–146.

[17] P.V. Thitame, and S.R. Shukla, Removal of lead (II) from synthetic solution and industry wastewater using almond shell activated carbon, *Environ. Prog. Sustain. Energy* 36 (2017) 1628–1633.

[18] Y.M. Ahmed, A. Al-Mamun, A. Khatib, M.R., Al, A.T. Jameel and M. AlSaadi, Efficient lead sorption from wastewater by carbon nanofibers, *Environ. Chem. Lett.* 13 (2015) 341–346.

[19] R.B. Onyancha, U.O. Aigbe, K.E. Ukhurebor, P.W. Muchiri, Facile synthesis and applications of carbon nanotubes in heavy-metal remediation and biomedical fields: a comprehensive review, *J. Mol. Struct.* 1238 (2021) 130462,

[20] T.S. Merjan, Z.T. Abd Ali, Green synthesis of bimetallic and trimetallic nanoparticles on glass granules for lead removal, *Desalin. Water Treat.* 322(2025) 101082.

[21] U.M. Ismail, A. I. Ibrahim, S.A. Onaizi, M. S. Vohra, Synthesis and application of MgCuAl-layered triple hydroxide/carboxylated carbon nanotubes/bentonite nanocomposite for the effective removal of lead from contaminated water, *Results Engin.* 24 (2024) 102991.

[22] J. Saini, V.K. Garg and R.K. Gupta, Green synthesized SiO<sub>2</sub>@OPW nanocomposites for enhanced Lead (II) removal from water, *Arab. J. Chem.* 13 (2020) 2496-2507.

[23] H.A. Sani, M.B. Ahmad, M.Z. Hussein, N.A. Brahim and T.A. Saleh, Nanocomposite of ZnO with montmorillonite for removal of lead and copper ions from aqueous solutions, *Process Saf. Environ. Protect.* 109 (2017) 97-105.

[24] X. Luo, X. Lei, X. Xie, B. Yu, N. Cai and F. Yu, Adsorptive removal of Lead from water by the effective and reusable magnetic cellulose nanocomposite beads entrapping activated bentonite, *Carbohyd. Polym.* 151(2016) 640-648.

[25] S. Wan, F. He, J. Wu, W. Wan, Y. Gu and B. Gao, Rapid and highly selective removal of lead from water using graphene oxide-hydrated manganese oxide nanocomposites, *J. Hazard. Mater.* 314 (2016) 32-40.

[26] T.A. Saleh, Nanocomposite of carbon nanotubes/silica nanoparticles and their use for adsorption of Pb (II): from surface properties to sorption mechanism, *Desalin. Water Treat.* 57(23)(2016) 10730-10744.

[27] R. Ansari, N. Khoshbakht Fahim, Application of polypyrrole coated on wood sawdust for removal of Cr(VI) ion from aqueous solutions, *React. Funct. Polym.* 67 (2007) 367-374

#### COPYRIGHTS



© 2022 by the authors. Licensee PNU, Tehran, Iran. This article is an open access article distributed under the terms and conditions of the Creative Commons Attribution 4.0 International (CC BY 4.0) (<http://creativecommons.org/licenses/by/4.0/>)

## نانو کامپوزیت پلی پیروول / سبوس برنج / $\text{Fe}_3\text{O}_4$ بعنوان یک جاذب برای حذف موثر

### سرب

محمد دانش پژوه\*

بخش شیمی، دانشگاه پیام نور، تهران، ایران

\* E-mail: fatemehsaber2003@pnu.ac.ir/ fatemehsaber2003@yahoo.com

تاریخ دریافت: ۱۴۰۳ تیر ۱۶ شهریور ماه ۱۴۰۳

#### چکیده

آلودگی عناصر سنگین خصوصا سرب رفتار ویژه ای بر روی سلامتی انسان و محیط زیست دارد. در این مطالعه نانو کامپوزیت پلی پیروول / سبوس برنج /  $\text{Fe}_3\text{O}_4$  (Rh/ppy) استر و برای حذف سرب از محیطهای آبی استفاده شد. در ابتدا نانوذره مغناطیسی  $\text{Fe}_3\text{O}_4$  با یک روش ساده و یک مرحله ای آماده و سپس پلی پیروول برای کارایی بیشتر جاذب به طریق شیمیایی بر روی سطح نانوذره قرار گرفت.  $\text{FeCl}_3$  بعنوان اکسید کننده برای اکسیداسیون پیروول استفاده شد. نانو کامپوزیت جدید توسط DLS و SEM و FT-IR مورد بررسی قرار گرفت. اثر pH، زمان تماس، مقدار جاذب، غلظت سرب، قدرت یونی و اثردما بر روی جذب سرب با درصد حذف ۹۹/۷ گردید. با استفاده از ثابت‌های تعادلی بدست آمده در دقیقه، غلظت اولیه  $30 \text{ ppm}$  تعیین گردید که منجر به بیشترین جذب سرب با درصد حذف ۹۹/۷ گردید. با استفاده از ثابت‌های تعادلی بدست آمده در دمای مختلط، پارامترهای ترمودینامیکی محاسبه شدند که بیانگر خودبخودی و گرمای بودن فرآیند جذب سرب می باشد. حداکثر ظرفیت جذب با استفاده از معادله لانگمویر  $85/47 \text{ میلی گرم بر گرم}$  محاسبه شد. داده های سینتیکی با شبه مرتبه دوم مطابقت داشتند.

کلید واژه ها: نانو کامپوزیت پلی پیروول / سبوس برنج /  $\text{Fe}_3\text{O}_4$ ، حذف، سرب